

Numerical Study Of Laminar Forced Convection Heat Transfer And Fluid Flow Characteristics In A Corrugated Channel

Waleed Mohammed Abed
Mechanical engineering Dept.
University of Anbar.

Mohammed Abed Ahmed
Mechanical engineering Dept.
University of Anbar.

Abstract

The problem of laminar forced convection heat transfer and fluid flow characteristics in a corrugated channel is studied numerically. The channel walls are maintained at constant temperature higher than fluid. The governing equations are written in two – dimensional Cartesian coordinates and solved by finite difference method with body fitted coordinates system (BFC) was used to stretch over the physical domain of the presented problem.

Effect of wavy angle and Reynolds number on heat transfer and fluid flow were studied. The solutions are carried for Reynolds numbers range from 500 to 2500, wavy angles range from 0° to 60° and Prandtl number is 0.71. The results have indicated that heat transfer and pressure drop increase with increasing wavy angle at same Reynolds numbers. The results are compared with previous experimental results and show good agreement.

Key words: Heat transfer characteristics, Laminar forced convection, Pressure drop, Corrugated channel

الخلاصة

تضمن البحث الحالي دراسة عددية لحل مشكلة انتقال الحرارة بالحمل القسري الطبقي وخصائص جريان المائع داخل مجرى متعرج. جدران المجرى ثابتة عند درجة حرارة أعلى من المائع. المعادلات الحاكمة كتبت بصيغة الإحداثيات الديكارتيه ثنائية البعد، ومن ثم تم حلها بطريقة الفروق المحددة باستخدام نظام مطابقة إحداثيات الجسم (BFC) ليغطي المجال الفيزيائي للمسألة الحالية.

تم دراسة تأثير زاوية التعرّيج ورقم رينولد على انتقال الحرارة والجريان. الدراسة العددية أنجزت على مدى رقم رينولد من 500 إلى 2500، زاوية التعرّيج من 0° إلى 60°، ورقم براندتل 0.71. بينت النتائج أن انتقال الحرارة والهبوط بالضغط يزدادان مع زيادة زاوية التعرّيج عند نفس رقم رينولد. عند مقارنة النتائج الحالية بالنتائج التجريبية السابقة كان هناك توافق جيد بينهما.

Nomenclature:

List of symbols

a	Amplitude,(m)
C_f	friction coefficient
D_h	hydraulic diameter,($2a+2H$), (m)
g	gravity acceleration,(m/s^2)
Nu	Nusselt number (h. D_h /k)
h	heat transfer coefficients, ($W/m^2 \cdot ^\circ C$)
H	height of channel, (m)
J	Jacobain of transformation
k	thermal conductivity , ($W/m \cdot ^\circ C$)
ΔP	Pressure drop,(Pa)
Pr	Prandtl number, (ν / α)
P	pitch, (m)
Re	Reynolds number, ($U_m \cdot D_h / \nu$)
L	long of corrugated channel, (m)
t	time, (s)
T	temperature, ($^\circ C$)
u ,v	velocities components,(m/s)
U, V	Dimensionless Velocity Component in ζ , and η -directions
U_m	mean velocity,(m/s)
x, y	Cartesian coordinates,(m)
X, Y	dimensionless Cartesian coordinates, ($X= x/ H$, $Y= y / H$)

Greek symbols

ζ, η	body-fitted coordinates
α	thermal diffusivity, $k/(\rho c_p)$ (m^2/s)
$\alpha', \beta', \lambda', \gamma'$	transforming coefficients
β	thermal expansion coefficient, (K^{-1})
ρ	density of fluid, (kg/m^3)
ν	kinematic viscosity, (m^2/s)
τ	dimensionless time, ($t \cdot U_m / H$)
λ	wavy angle
ψ	stream function
Ψ	dimensionless stream function, ($\psi / H \cdot U_m$)
Ω	vorticity, ($1/s$)
ω	dimensionless vorticity, ($\Omega \cdot H$) / U_m
θ	dimensionless temperature, $(T - T_b) / (T_w - T_b)$

Subscripts

b	bulk
f	fluid
l	lower plate
u	upper plate
w	wall
c	corrugated channel
p	plain channel

1. Introduction:

Heat exchangers are being used in many industrial applications, such as manufacturing, chemical process, and recycling. Under the principles of heat recovery and temperature difference, several types of heat exchangers are developed. Among them, plate heat exchangers probably are the most common ones in the manufacturing industry because of their compact and easy upgradeable structures. Basic channel geometry used in plate heat exchangers is corrugated duct because of their efficient heat exchange capabilities. This efficiency is attributed to the pattern of heat transfer plates which produce turbulence at low fluid velocities. The abrupt changes in direction and velocities when the fluid flows through narrow plate pattern help produce turbulence. This turbulence, created by the shape of the plate pattern, reduces the liquid film resistance to heat transfer more efficiently than turbulence created by high flow rates and pressures in conventional exchangers.

There are many researchers have investigated flow and heat transfer through corrugated channel numerically and experimentally. Focke et al. (1985) [1] investigated the inclination angle between plate corrugations and the overall flow direction is a major parameter in the thermal-hydraulic performance of plate heat exchangers. The observed maximum transfer rate at an angle of about 80° is explained from the observed flow patterns. At higher angles the flow pattern becomes less effective for transfer, in particular at 90° marked flow separation is observed. Tanda and Vittori (1996) [2] have numerically investigated laminar fully developed flow and heat transfer in a two dimensional wavy channel characterized by a wavy wall, heated at uniform heat flux, and an opposite wall that is flat and adiabatic. They found that the pressure drop in this wavy channel was always higher than the corresponding straight duct, while heat transfer performance tended to decrease or increase depending on the geometry of the wavy plate, Reynolds number and Prandtl number.

Rush et al. (1999) [3] experimentally investigated local heat transfer and flow behavior for laminar and transitional flows in sinusoidal wavy passages. Flow visualization methods were used to characterize the flow field and detect the onset of macroscopic mixing. The entire channel exhibited unsteady, macroscopic mixing at $Re \approx 1600$ and the onset of this mixing is linked directly to the significant increases in local heat transfer. Blomerius and Mitra (2000) [4] studied fluid flow and heat transfer in corrugated ducts have been investigated from the numerical solutions of the Navier-Stokes equations in the range of Reynolds number (600-2000). The angles 45° and 90° between the corrugations and the main stream direction have been considered.

Kundu (2001) [5] studied numerical solutions for laminar forced convection in two-dimensional and three-dimensional sinusoidal corrugated ducts, which are maintained at uniform wall temperature or uniform heat flux, are considered. For the two-dimensional problem, numerical solutions are obtained for different corrugation aspect ratios, plate spacing ratio, flow rates.

For the three-dimensional problem, different cross-stream aspect ratios are also considered. The vortices strength increases with increasing Reynolds number and decreases with increasing wall separation. This cross-stream longitudinal recirculation further increases the overall heat transfer coefficient. Both friction factor and Nusselt number results are presented for different aspect ratios and plate spacing ratio in the two-dimensional case, as well as for different cross-stream aspect ratios in the three dimensional case, for a wide range of flow conditions ($50 < Re < 1000$) that highlight the enhanced thermal-hydraulic behavior of corrugated channels.

Hossain and Islam 2004 [6] investigated the fluid flow and heat transfer characteristic in corrugated channel numerically with two different types of surface waviness one sinusoidal channel and another triangular channel. The results show that these types of wavy channel increase heat transfer by mixing the fluid near the wall with main flow due to vortex, also increase friction factor.

Paisarn N. (2007) [7] experimentally studied The heat transfer characteristics and pressure drop in the channel with V-corrugated upper and lower plates under constant heat flux as shown in Fig. 1. The test section is the channel with two opposite corrugated plates on which all configuration peaks lie in a staggered arrangement. He is tested corrugated plates with three different corrugated tile angles of 20° , 40° and 60° . The experiments are performed for Reynolds number ranges of 2000–9000. He showed effect corrugated surface on the enhancement of heat transfer and pressure drop. The heat transfer coefficients obtained from the channel with the corrugated surface are higher than those with the plain surface. The pressure drop also increases.

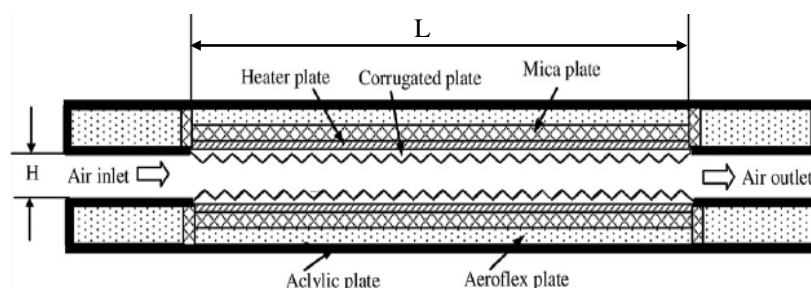


Fig. 1 Schematic diagram of experimental test section

Wahad and Yousif (2008) [8] investigated the fully developed laminar forced convective heat transfer and fluid flow characteristics inside two dimensional triangular wavy channels. Calculations were performed for Reynolds number range of ($50 \leq Re \leq 1000$). They showed that the heat transfer and pressure drop increase with increasing Reynolds number and depended strongly on triangular wavy dimensions, also heat transfer enhancement when fluid flow through triangular wavy channel when compare the results with straight channel.

In the present paper, a numerical investigation is described on studying of laminar forced convection heat transfer and fluid flow with using V-corrugated channel with corrugated angles from 0° to 60° and Reynolds number from 500 to 2500. The effects of various relevant parameters on the heat transfer and pressure drop characteristics are also investigated.

2. Problem Description:

The present paper studied the problem of laminar forced convection in a horizontal corrugated channel. The channel is composed of two corrugated plates separated by a distance (H) in y - direction, the height of wavy ,amplitude, (a) , wavy angle (λ) and wavy pitch (P). The length of corrugated channel (L) in x - direction. The channel walls are at uniform temperature (T_h) and no- slip boundaries. The flow is steady, laminar, incompressible and two dimension. The geometry and coordinate system is shown in Fig. 2.

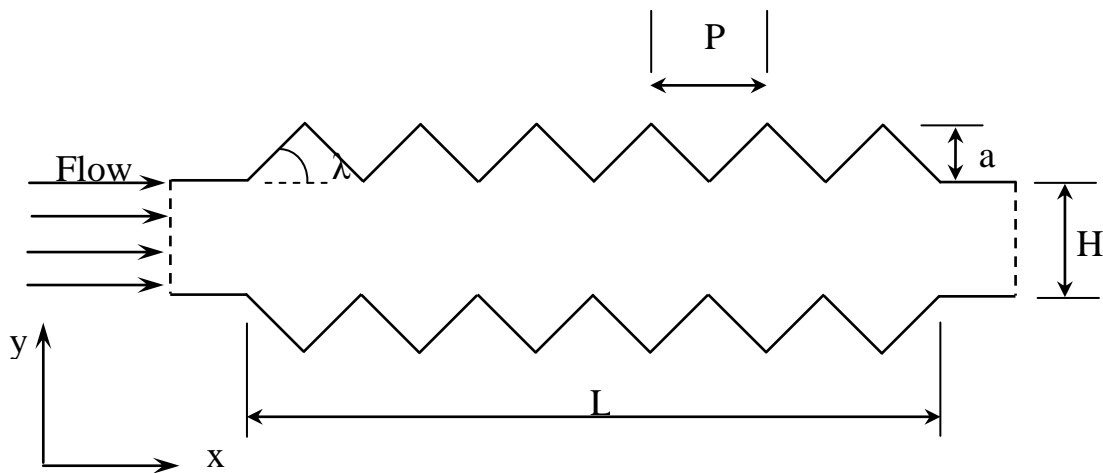


Fig. 2 Schematic diagram of the corrugated channel

3. Governing Equations:

The governing equations of continuity, momentum, and energy can be written as [5, 8]:

$$\frac{\partial u}{\partial x} + \frac{\partial v}{\partial y} = 0 \quad \dots(1)$$

$$\frac{\partial u}{\partial t} + u \frac{\partial u}{\partial x} + v \frac{\partial u}{\partial y} = -\frac{1}{\rho} \frac{\partial p}{\partial x} + \nu \left(\frac{\partial^2 u}{\partial x^2} + \frac{\partial^2 u}{\partial y^2} \right) \quad \dots(2)$$

$$\frac{\partial v}{\partial t} + u \frac{\partial v}{\partial x} + v \frac{\partial v}{\partial y} = -\frac{1}{\rho} \frac{\partial p}{\partial y} + \nu \left(\frac{\partial^2 v}{\partial x^2} + \frac{\partial^2 v}{\partial y^2} \right) \quad \dots(3)$$

$$\frac{\partial T}{\partial t} + u \frac{\partial T}{\partial x} + v \frac{\partial T}{\partial y} = \alpha \left(\frac{\partial^2 T}{\partial x^2} + \frac{\partial^2 T}{\partial y^2} \right) \quad \dots(4)$$

The vorticity-stream function method will be used in the solution to obtain two equation are vorticity transport and stream function equations in dimensionless form are:

$$\frac{\partial^2 \Psi}{\partial X^2} + \frac{\partial^2 \Psi}{\partial Y^2} = -\omega \quad \dots(5)$$

$$\frac{\partial \omega}{\partial \tau} + \frac{\partial \Psi}{\partial Y} \frac{\partial \omega}{\partial X} - \frac{\partial \Psi}{\partial X} \frac{\partial \omega}{\partial Y} = \frac{1}{\text{Re}} \left(\frac{\partial^2 \omega}{\partial X^2} + \frac{\partial^2 \omega}{\partial Y^2} \right) \quad \dots(6)$$

On the other hand, the energy equation in dimensionless form is:

$$\frac{\partial \theta}{\partial \tau} + \frac{\partial \Psi}{\partial Y} \frac{\partial \theta}{\partial X} - \frac{\partial \Psi}{\partial X} \frac{\partial \theta}{\partial Y} = \frac{1}{\text{Pe}} \left(\frac{\partial^2 \theta}{\partial X^2} + \frac{\partial^2 \theta}{\partial Y^2} \right) \quad \dots(7)$$

4. Coordinate Transformation:

Due to curvilinear geometry of the boundary, a system of general coordinate has been adopted here in order to obtain a computationally convenient representation of the physical domain. If x and y are set as physical domain and ζ and η as computational domain, the relationships of x , y and ζ , η for the present study are as follows:

$$\zeta = \zeta(x, y) \quad \dots(8a)$$

$$\eta = \eta(x, y) \quad \dots(8b)$$

With the above, the governing equations are expressed as :

$$\lambda' \cdot \frac{\partial \Psi}{\partial \zeta} + \sigma' \cdot \frac{\partial \Psi}{\partial \eta} + \alpha' \cdot \frac{\partial^2 \Psi}{\partial \zeta^2} - 2\beta' \cdot \frac{\partial^2 \Psi}{\partial \zeta \partial \eta} + \gamma' \cdot \frac{\partial^2 \Psi}{\partial \eta^2} = -\omega \cdot J^2 \quad \dots(9)$$

$$\frac{\partial \omega}{\partial \tau} + \frac{1}{J} \left(-\frac{\partial \Psi}{\partial \zeta} \cdot \frac{\partial \omega}{\partial \eta} + \frac{\partial \Psi}{\partial \eta} \cdot \frac{\partial \omega}{\partial \zeta} \right) = \frac{1}{(J^2 \cdot \text{Re})} \left(\lambda' \cdot \frac{\partial \Psi}{\partial \zeta} + \sigma' \cdot \frac{\partial \Psi}{\partial \eta} + \alpha' \cdot \frac{\partial^2 \Psi}{\partial \zeta^2} - 2\beta' \cdot \frac{\partial^2 \Psi}{\partial \zeta \partial \eta} + \gamma' \cdot \frac{\partial^2 \Psi}{\partial \eta^2} \right) \quad \dots(10)$$

$$\frac{\partial \theta}{\partial \tau} + \left(-\frac{\partial \Psi}{\partial \zeta} \cdot \frac{\partial \theta}{\partial \eta} + \frac{\partial \Psi}{\partial \eta} \cdot \frac{\partial \theta}{\partial \zeta} \right) / J = \left(\lambda' \cdot \frac{\partial \theta}{\partial \zeta} + \sigma' \cdot \frac{\partial \theta}{\partial \eta} + \alpha' \cdot \frac{\partial^2 \theta}{\partial \zeta^2} - 2\beta' \cdot \frac{\partial^2 \theta}{\partial \zeta \partial \eta} + \gamma' \cdot \frac{\partial^2 \theta}{\partial \eta^2} \right) / (J^2 \cdot \text{Pe}) \quad \dots(11)$$

Where J is the Jacobian of the transformation and $\lambda', \sigma', \alpha', \beta'$ and γ' are the coefficients of coordinate transformation.

After transform the governing equations from physical domain into computational domain, the vorticity transport and energy equations are solved by explicit method of finite difference based on the time marching technique. On the other hand, the stream function equation is solved by relaxation method. The computational domain covers a region that extends 300 mm in x-direction and 20mm in y- direction. A uniform grid, 300×20, in the transformed computational domain was considered suitable for covering the computational domain (see Fig.3).

The corresponding boundary conditions used for computations are given as follows:

At the inlet $\theta = 0, \Psi = y,$ and $\omega = 0 \quad \dots(12a)$

Along lower corrugated plate $\Psi = -1, \theta = 1, \omega = -\frac{\partial U}{\partial Y} \quad \dots(12b)$

Along upper corrugated plate $\Psi = 1, \theta = 1, \omega = -\frac{\partial U}{\partial Y} \quad \dots(12c)$

At the exist $\frac{\partial \Psi}{\partial X} = \frac{\partial \theta}{\partial X} = \frac{\partial \omega}{\partial X} = 0 \quad \dots(12d)$

5. Local and the Average Nusselt Numbers:

The heat transfer across the horizontal corrugated channel is expressed in terms of local and mean Nusselt numbers. The local Nusselt number for corrugated plate is

$$Nu = -\frac{\partial T}{\partial y} = -\frac{D_h}{H} \frac{\partial \theta}{\partial Y} \quad \dots(13)$$

In terms the new coordinates, the Nusselt number in above equation can be rewritten as follows [9]:

$$Nu = -\frac{D_h}{H} \frac{1}{J\sqrt{\gamma'}} \left(\gamma' \cdot \frac{\partial \theta}{\partial \eta} - \beta' \cdot \frac{\partial \theta}{\partial \xi} \right) \quad \dots(14)$$

Since the temperature along the wall of plate is constant Eq.(14) becomes :

$$Nu = -\frac{D_h}{H} \frac{\gamma'}{J\sqrt{\gamma'}} \frac{\partial \theta}{\partial \eta} \Big|_w \quad \dots(15)$$

Now, the local Nusselt number for the lower plate is :

$$Nu_l = -\frac{D_h}{H} \frac{\gamma'}{J\sqrt{\gamma'}} \frac{\partial \theta}{\partial \eta} \Big|_{\eta=0} \quad \dots(16)$$

and, the local Nusselt number for the upper plate is :

$$Nu_u = -\frac{D_h}{H} \frac{\gamma'}{J\sqrt{\gamma'}} \frac{\partial \theta}{\partial \eta} \Big|_{\eta=1} \quad \dots(17)$$

On the other hand, the average Nusselt, for corrugated channel is [10]:

$$Nu = -\frac{1}{L} \frac{D_h}{H} \frac{\gamma'}{J\sqrt{\gamma'}} \int_0^L \left[\frac{\partial \theta}{\partial \eta} \Big|_{\eta=0} + \frac{\partial \theta}{\partial \eta} \Big|_{\eta=1} \right] .dx \quad \dots(18)$$

6. Friction Coefficient and Pressure Drop:

The local friction coefficient for the flow in a corrugated channel is defined by:

$$C_f = 2 \frac{D_h}{H} \frac{1}{\text{Re}} \frac{\partial U}{\partial Y} = -2 \frac{D_h}{H} \frac{1}{\text{Re}} \omega \Big|_w \quad \dots(19)$$

Now, the local friction coefficient for the lower plate is :

$$C_{fL} = -2 \frac{D_h}{H} \frac{1}{\text{Re}} \omega \Big|_{\eta=0} \quad \dots(20)$$

The local friction coefficient for the upper plate is :

$$C_{fu} = -2 \frac{D_h}{H} \frac{1}{\text{Re}} \omega \Big|_{\eta=1} \quad \dots(21)$$

The average value of friction coefficient for corrugated channel is :

$$C_f = -\frac{2}{L} \frac{D_h}{H} \frac{\gamma'}{J\sqrt{\gamma'}} \frac{1}{\text{Re}} \int_0^L [\omega|_{\eta=0} + \omega|_{\eta=1}] dx \quad \dots(22)$$

Also, the pressure drop in a corrugated channel is

$$\Delta P = \frac{C_f}{4} \frac{L}{D_h} \frac{\rho u^2}{2g} \quad \dots(23)$$

7. Resulted and Discussion:

Numerical solutions achieved for Reynolds number range (500, 1000, 1500, 2000, 2500), wavy angles range (0°, 10°, 20°, 30°, 40°, 60°), and Prandtl number is kept at 0.71. Compare results against the experimental work of Paisarn N. [7] to validate the present model. Figs. 4 and 5 shows that the average Nusselt numbers obtained in the present study are in good agreement with those obtained by Paisarn N. [7].

Fig. (6) Shows streamline contours for air flow in a corrugated channel at Reynolds number 500, and with different wavy angles. When the fluid flowing in a corrugated channel, the flow separation occurs in cavities and recirculation region tends to grow laterally along channel wall in cavities.

It is also seen that as wavy angles (λ) increase, the number of cavities in a corrugated channel increased and size of cavities decrease. The isotherm line contours in a corrugated channel at Reynolds number 500 for different wavy angles is shown in Fig.(7). It is found that, the temperature gradient at right side in cavity is larger than that at another side. This is due to the fact that interaction of the core fluid with the fluid in the cavities replenishes the thermal boundary and results in enhanced heat transfer. The corresponding velocity vector at same Reynolds number is shown in Fig.(8). The onset and growth of recirculation zones promote the mixing of fluid in the boundary layer, thereby enhancing convection heat transfer.

Fig. 9 gives the variation of the average Nusselt number with Reynolds number for the different wavy angles. It is clear from figure, the average Nusselt number increase with increasing Reynolds number and wavy angles (λ). It can be seen clearly from the figure that the Nusselt numbers at higher wavy angle are higher than those at lower ones. Figs. (10 and 11) depict the ratio of average Nusselt and pressure drop for corrugated channel to that for plain channel with Reynolds number for the different wavy angles. It is found that the enhancement ratio, (Nu_c / Nu_p), tends to increase as wavy angle increase, this is due to re-circulation zones along corrugated channel. This effect decrease with increasing Re, this is because of the strength of re-circulation zones increase with increasing Re. The corresponding pressure drop increase with increasing wavy angle at the same Reynolds numbers.

It is also found from Figs. (10 and 11), the maximum enhancement in heat transfer occurs at $\lambda = 60^\circ$ is (4.02) for all values of Reynolds numbers, but the maximum pressure drop (2.2) and consequently large value of pumping power.

8. Conclusions:

Laminar forced convection in a corrugated channel has been studied numerically by finite difference method. The present results agree very well with the previous experimental study by Paisarn N. (2007) [7]. The results give detailed analysis of the average Nusselt number and pressure drop with different Reynolds number and wavy angles. It is found that the optimum values of the heat transfer enhancement and pressure drop are (3.6) and (1.11) times higher than those from the plane channel at wavy angle ($\lambda = 40^\circ$), respectively.

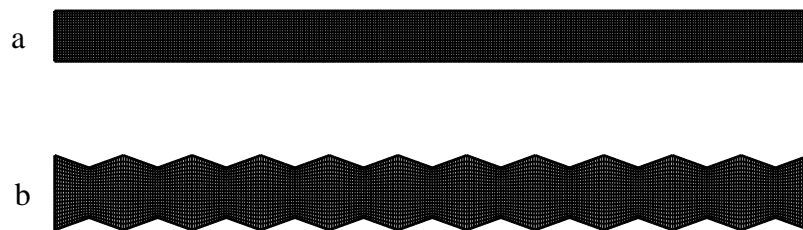


Fig.3 computational grid (a) $\lambda=0^\circ$ (plain channel), (b) $\lambda=20^\circ$ (corrugated channel)

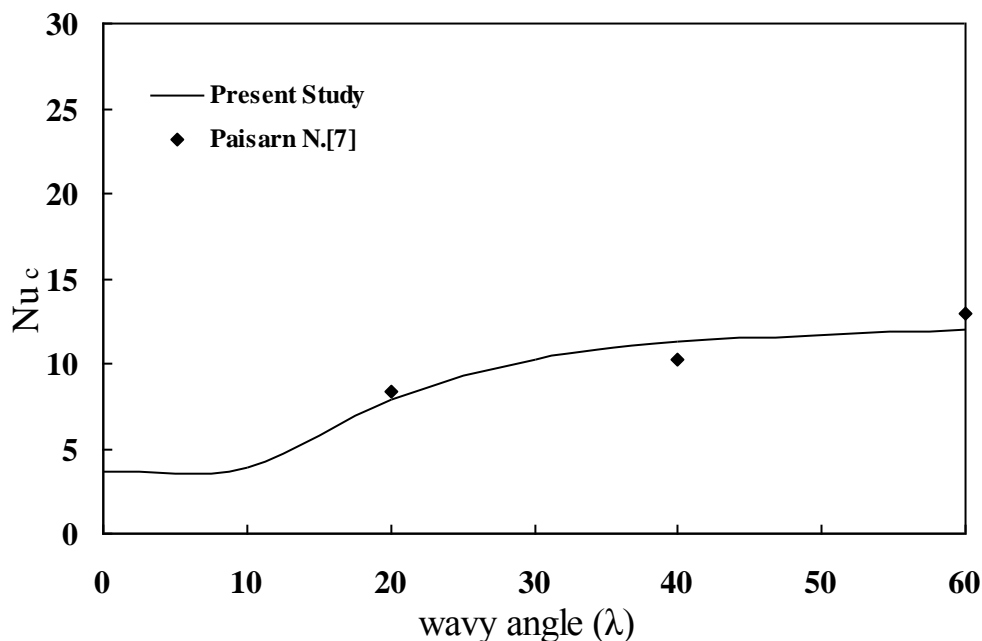


Fig. 4 Comparison between present study and previous experimental results at $Re = 2500$

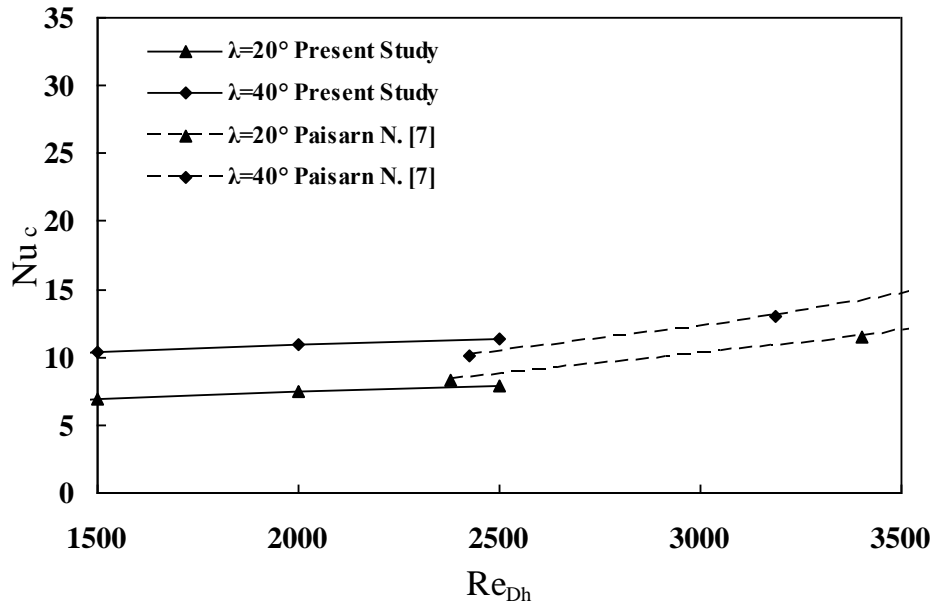


Fig.5 Comparison between present study and previous experimental results for different wavy angles

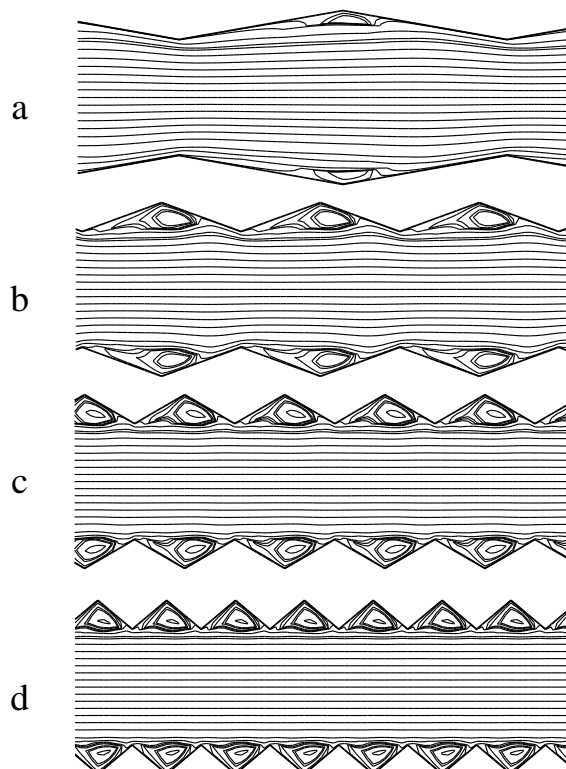


Fig.6 Streamline counter at $Re=500$ for different wavy angles

(a) $\lambda=10^\circ$, (b) $\lambda=20^\circ$, (c) $\lambda=30^\circ$, (d) $\lambda=40^\circ$

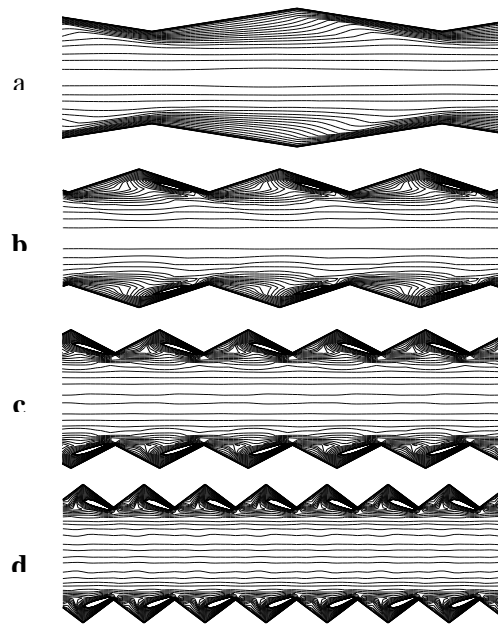
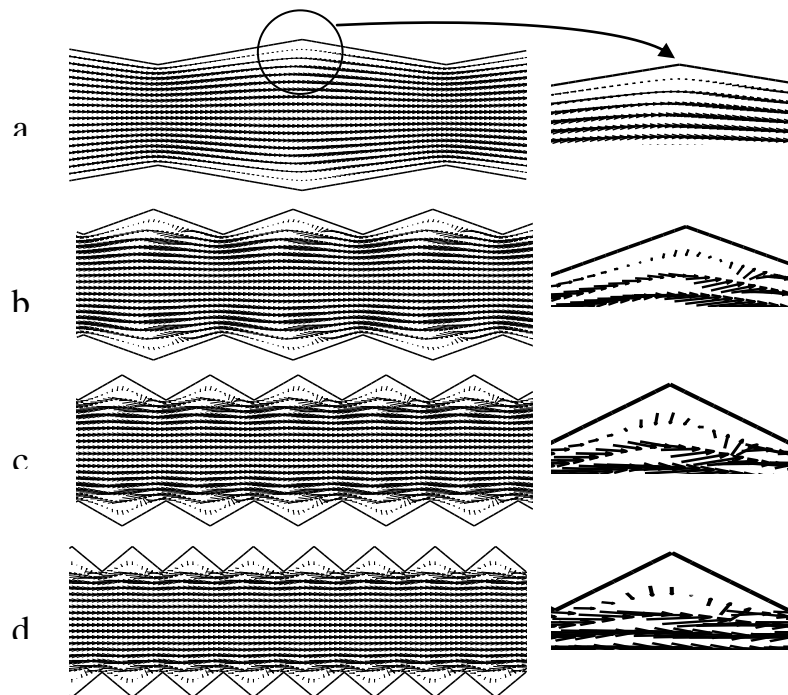


Fig.7 Dimensionless temperature counter at $Re=500$. for different wavy angles



**Fig. 8 Velocity vector counter at $Re = 500$.
(a) $\lambda=10^\circ$, (b) $\lambda=20^\circ$, (c) $\lambda=30^\circ$, (d) $\lambda=40^\circ$**

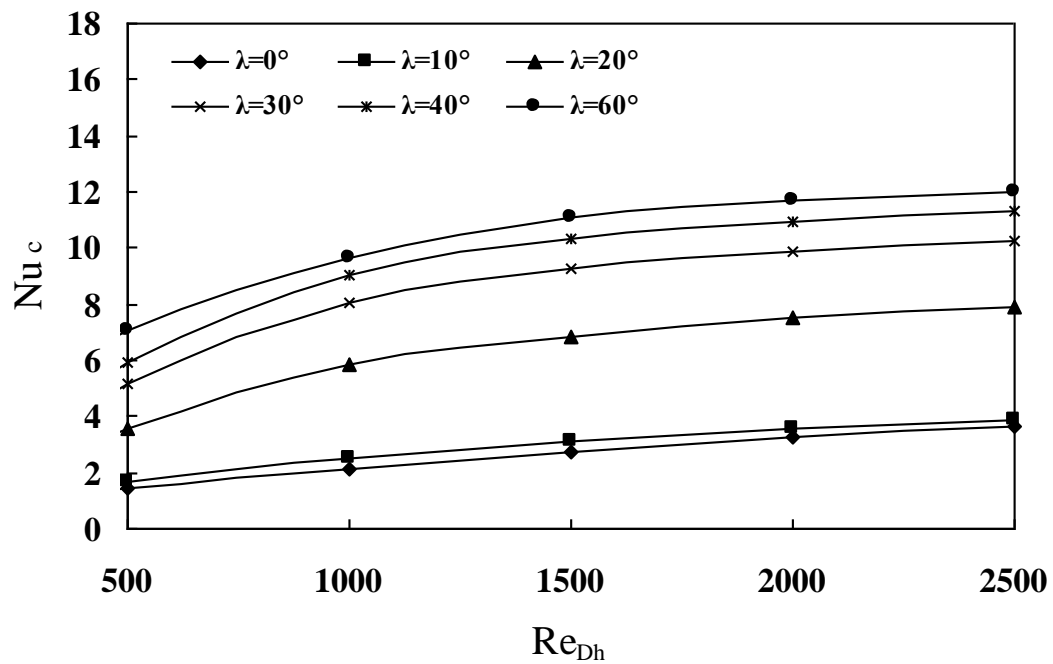


Fig. 9 Variation of average Nusselt number with Reynolds number for different wavy angles

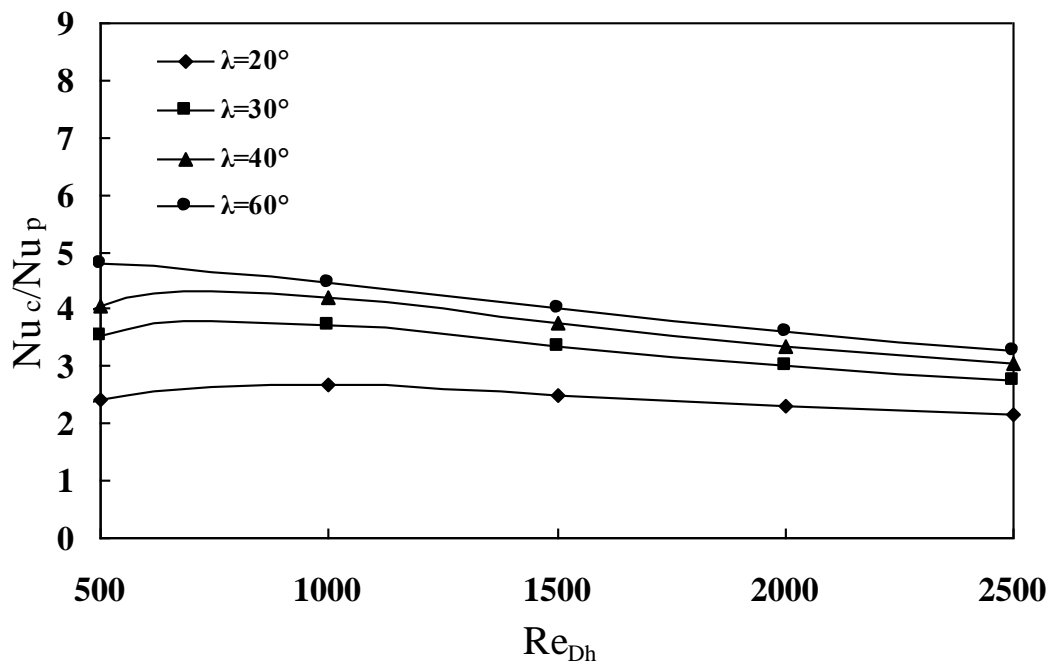


Fig. 10 Ratio of the average Nusselt number for corrugated channel to the average Nusselt number for plain channel with Reynolds number for different wavy angle

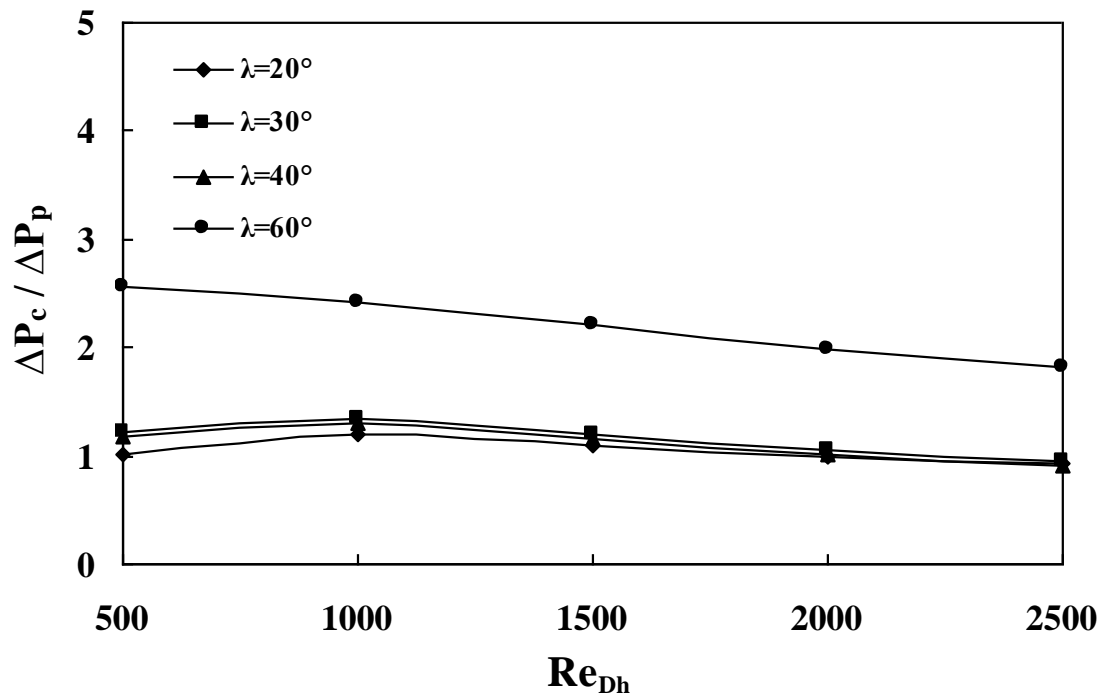


Fig. 11 Ratio of the pressure drop for corrugated channel to the pressure drop for plain channel with Reynolds number for different wavy angles

9. References:

- [1] Focke, W. W., Zachariades, J. & Olivier, I. “*The effect of the corrugation inclination angle on the thermohydraulic performance of plate heat exchangers*”, Int. J. Heat Mass Transfer. Vol. 28, No. 8, pp. 1469 - 1479, 1985.
- [2] Tanda, G. & Vittori, G. “*Fluid Flow and Heat Transfer in Two-Dimensional Wavy Channel*” Int. J. Heat Mass Transfer. Vol. 31, No. 6, pp. 411- 418, 1996.
- [3] Rush, T. A., Newell, T. A. & Jacobi, A. M. “*An Experimental Study of Flow and Heat Transfer in Sinusoidal Wavy Passages*” *Int. Journal of Heat and Mass Transfer*, Vol. 42, pp. 1541-1553, 1999.
- [4] Blomerius, H. & Mitra, N. K. “*Numerical Investigation of Convective Heat Transfer and Pressure Drop in Wavy Duct*” *Numerical Heat Transfer, Part A*, 37:37-54, 2000.
- [5] Kundu, J. “*Numerical Investigation of Laminar Forced Convection in Two- Dimensional and Three-Dimensional Sinusoidal Corrugated Ducts*” M. Sc. In Mechanical Engineering thesis, Engineering College - University of Cincinnati, 2001.
- [6] Hossain, M. Z. & Islam, A. K. M. S. “*Numerical Investigation of Unsteady Flow and Heat Transfer in Wavy Channels*” 15th Australasian fluid mechanics conference the university of Sydney, Sydney, Australia 13-17 December, 2004.
- [7] Paisarn, N. “*Heat Transfer Characteristics and Pressure Drop in Channel with V-Corrugated Upper and Lower Plates*” *Energy Conversion and Management*, Vol. 48, Issue 5, pp. 1516-1524, 2007.
- [8] Wahad, M & Yousif, A. H. “*A Numerical Investigation of Fluid Flow and Heat Transfer Characteristics inside a Wavy Channel*” First Scientific Conference Technical College-Najaf, Najaf , Iraq, 16-17 March, 2008.
- [9] Broughton, R. C. & Oliver, A. J. “*A Numerical Model for Convection in Complex-Dimensional Geometries and it is Application to Buoyancy flow in Power Cable*” *International Heat Transfer Conferences*, vol. 2, pp. 447 - 451, 1986.
- [10] AL-Khafaji, A. W. & Tooley, J. R. “*Numerical Methods in Engineering Practice*” 1st Edition, CBS Publishing, Japan Ltd, 1986.